vanishing white matter disease resembling Creeleukoencephalopathy.	Anzai R, Okuda M, Iai M, Yamashita S, Okabe T, Aida N, Tsurusaki Y, Saitsu H, Matsumoto N, Osaka H.	doi:10.1016/j.braindev.2014.10.002. [Epub ahead of print]		
Intracranial Hemorrhage andTortuosity of Veins Detected on Susceptibility-weighted Imaging of a Child with a Type IV Collagen α1 Mutation and Schizencephaly.	Niwa T, Aida N, Osaka H, Wada T, Saitsu H, Imai Y.	Magn Reson Med Sci. 2014Dec15. [Epub ahead of print]	2014	国外
大脳萎縮症	小坂　仁	新領域別症候群シリーズ No.29「神経症候群（第２版）IV、日本臨牀社 p.319-324. 2014	2014	国内
小脳萎縮症	小坂　仁	新領域別症候群シリーズ No.29「神経症候群（第２版）IV、日本臨牀社 p.325-328. 2014	2014	国内
Intra-Amniotic rAAV-Mediated Microdystrophin Gene Transfer Improves Canine X-Linked Muscular Dystrophy and May Induce Immune Tolerance	Hayashita-Kinoh H, Okada H, Nitahara-Kasahara Y, Chiyo T, Yugeta N, Okada T, Takeda S	Mol Ther, 2015, in press	2015	国外
Fukutin is prerequisite to ameliorate muscular dystrophic phenotype by myofiber-selective LARGE expression.	Ohtsuka Y, Kanagawa M, Yu CC, Ito C, Chiyo T, Kobayashi K, Okada T, Takeda S and Toda T	Sci Rep., 2015, in press	2015	国外
DOK7 gene therapy benefits mouse models of diseases characterized by defects in the neuromuscular junction	Arimura S, Okada T, Tezuka T, Chiyo T, Nitahara-Kasahara Y, Yoshimura T, Motomura M, Yoshida N, Beeson D, Takeda S and Yamanashi Y	Science, 345(6203):1505-8	2014	国外
Reward-timing-dependent bidirectional modulation of cortical microcircuits	Hira R, Ohkubo F, Masamizu Y, Ohkura M, Nakai J, Okada T	Nat Commun., in press	2014	国外

during optical single-neuron operant conditioning	and Matsuzaki M.			
Two distinct layer-specific dynamics of cortical ensembles during learning of a motor task.	Masamizu Y, Tanaka YR, Tanaka YH, Hira R, Kitamura K, Isomura Y, Okada T and Matsuzaki M	Nat Neurosci, 17(7):987-94	2014	国外
Two distinct layer-specific dynamics of cortical ensembles during learning of a motor task.	Masamizu Y, Tanaka YR, Tanaka YH, Hira R, Kitamura K, Isomura Y, Okada T and Matsuzaki M	Nat Neurosci, 17(7):987-94	2014	国外
Dystrophic mdx mice develop severe cardiac and respiratory dysfunction following genetic ablation of the anti-inflammatory cytokine IL-10	Nitahara-Kasahara Y, Hayashita-Kinoh H, Chiyo T, Nishiyama A, Okada H, Takeda S and Okada T	Hum Molecular Genetics, 23(15):3990-4000	2014	国外
Cell therapeutic approaches using multipotent mesenchymeal stromal cells for muscular dystrophy.	Nitahara-Kasahara Y, Takeda S and Okada T	Inflammation and Regeneration, in press	2014	国内
West Syndrome in a Patient With Schinzel-Giedion Syndrome.	Miyake F, Kuroda Y, Naruto T, Ohashi I, Takano K, Kurosawa K.	J Child Neurol. in press	2014	国外
ゲノムデータベースの利用	黒澤健司	医学のあゆみ 250:349-352.	2014	国内
Different patterns of hypomyelination and cerebellar abnormality between POLR3A and POLR3B mutations.	Takanashi J, Osaka H, Saitsu H, Sasaki M, Mori H, Shibayama H, Tanaka M, Nomura Y, Terao Y, Barkovich AJ	Brain Dev 2014; 36: 259-263	2014	国外
Neurochemistry in Shiverer mouse depicted on MR spectroscopy.	Takanashi J, Nitta N, Iwasaki N, saito S, Tanaka R, Aoki I.	J Magn Reson Imaging 2014; 39: 1550-1557	2014	国外
MR spectroscopy in 18q-syndrome suggesting other than hypomyelination.	Tada H, Takanashi J	Brain Dev 2014; 36: 57-60.	2014	国外
Pontine malformation, undecussated pyramidal tracts, and regional polymicrogyria: a new syndrome.	Irahara K, Saito Y, Sugai K, Nakagawa E, Saito T, Komaki H, Nakata Y, Sato N, Baba K, Yamamoto T, Chan WM, Andrews C, Engle EC, Sasaki M.	Pediatr Neurol 50: 384-8, 2014.	2014	国外

Mild developmental delay and obesity in two patients with mosaic 1p36 deletion syndrome.	Shimada S, Maegaki Y, Osawa M, Yamamoto T.	Am J Med Genet A 164A: 415-420, 2014.	2014	国外
Narrowing of the responsible region for severe developmental delay and autistic behaviors in WAGR syndrome down to 1.6 Mb including PAX6, WT1, and PRRG4.	Yamamoto T, Togawa M, Shimada S, Sangu N, Shimojima K, Okamoto N.	Am J Med Genet A 164A: 634-638, 2014.	2014	国外
Growth patterns of patients with 1p36 deletion syndrome.	Sangu N, Shimojima K, Shimada S, Ando T, Yamamoto T.	Congenit Anom (Kyoto) 54: 82-86, 2014.	2014	国外
Epidemiological, clinical, and genetic landscapes of hypomyelinating leukodystrophies.	Numata Y, Gotoh L, Iwaki A, Kurosawa K, Takanashi J, Deguchi K, Yamamoto T, Osaka H, Inoue K.	J Neurol 261: 752-758, 2014.	2014	国外
Overlapping microdeletions involving 15q22.2 narrow the critical region for intellectual disability to NARG2 and RORA.	Yamamoto T, Mencarelli MA, Di Marco C, Mafalda M, Vascotto M, Balestri P, Gérard M, Mathieu-Dramard M, Andrieux J, Breuning M, Hoffer MJV, Ruivenkamp CAL, Shimada S, Sangu N, Shimojima K, Umezu R, Kawame H, Matsuo M, Saito K, Renieri A, Mari F.	Eur J Med Genet 57: 163-168, 2014.	2014	国外
An emerging phenotype of Xq22 microdeletions in females with severe intellectual disability, hypotonia, and behavioral abnormalities.	Yamamoto T, Wilsdon A, Joss S, Isidor B, Erlandsson A, Suri M, Sangu N, Shimada S, Shimojima K, Le Caignec C, Samuelsson L, Stefanova M.	J Hum Genet 59: 300-306, 2014.	2014	国外
Novel compound heterozygous mutations of POLR3A revealed by whole-exome sequencing in a patient with hypomyelination.	Shimojima K, Shimada S, Tamasaki A, Akaboshi S, Komoike Y, Saito A, Furukawa T, Yamamoto T.	Brain Dev 36: 315-321, 2014.	2014	国外
Whole-exome sequencing identifies a de novo	Shimojima K, Narita A, Maegaki Y, Saito	BMC Res Notes 7: 465, 2014.	2014	国外

TUBA1A mutation in a patient with sporadic malformations of cortical development: a case report.	A, Furukawa T, Yamamoto T.			
SLC16A2 mutations in two Japanese patients with Allan-Herndon-Dudley syndrome.	Yamamoto T, Shimojima K, Umemura A, Uematsu M, Nakayama T, Inoue K.	Hum Genome Variation 1: 14010, 2014.	2014	国外
MLC1 mutations in Japanese patients with megalencephalic leukoencephalopathy with subcortical cysts.	Shimada S, Shimojima K, Masuda T, Nakayama Y, Kohji T, Tsukamoto H, Matsubasa T, Oka A, Yamamoto T.	Hum Genome Variation 1: 14019, 2014.	2014	国外
Bilateral periventricular nodular heterotopia with megalencephaly: a case report.	Abe Y, Kobayashi S, Wakusawa K, Tanaka S, Inui T, Yamamoto T, Kunishima S, Haginoya K.	J Child Neurol 29: 818-822, 2013	2014	国外
A de novo TUBB4A mutation in a patient with hypomyelination mimicking Pelizaeus-Merzbacher disease.	Shimojima K, Okumura A, Ikeno M, Nishimura A, Saito A, Saitsu H, Matsumoto N, Yamamoto T.	Brai Dev 37 :281-5, 2015.	2014	国外
Microarray analysis of 50 patients reveals the critical chromosomal regions responsible for 1p36 deletion syndrome-related complications.	Shimada S, Shimojima K, Okamoto N, Sangu N, Hirasawa K, Matsuo M, Ikeuchi M, Shimakawa S, Shimizu K, Mizuno S, Kubota M, Adachi M, Saito Y, Tomiwa K, Haginoya K, Numabe H, Kako Y, Hayashi A, Sakamoto H, Hiraki Y, Minami K, Takemoto K, Watanabe K, Miura K, Chiyonobu T, Kumada T, Imai K, Maegaki Y, Nagata S, Kosaki K, Izumi T, Nagai T, Yamamoto T.	Brain Dev [Early on-line view]	2014	国外
A case of pontine tegmental cap dysplasia with comorbidity of	Chong PF, Haraguchi K, Torio M, Kirino M, Ogata R,	Brain Dev [Early on-line	2014	国外

oculoauriculovertebral spectrum.	Matsukura M, Sakai Y, Ishizaki Y, Yamamoto T, Kira R.	view].		
Clinical course and images of four familial cases of Allan-Herndon-Dudley syndrome with a novel monocarboxylate transporter 8 gene mutation.	Kobayashi S, Onuma A, Inui T, Wakusawa K, Tanaka S, Shimojima K, Yamamoto T, Haginoya K.	Pediatr. Neurol [Early on-line view]	2014	国外
Neuropsychological profiles of patients with 2q37.3 deletion associated with developmental dyspraxia.	Ogura K, Takeshita K, Arakawa C, Shimojima K, Yamamoto T.	Am J Med Genet B 165B: 684-90, 2014.	2014	国外
Clinical impacts of genomic copy number gains at Xq28.	Yamamoto T, Shimojima K, Shimada S, Yokochi K, Yoshitomi S, Yanagihara K, Imai K, Okamoto N.	Hum Genome Variation 1: 14001, 2014.	2014	国外
A novel KCNT1 mutation in a Japanese patient with epilepsy of infancy with migrating focal seizures.	Shimada S, Hirano Y, Ito S, Oguni H, Nagata S, Shimojima K, Yamamoto T.	Hum Genome Variation 1: 14027, 2014.	2014	国外
3p interstitial deletion including PRICKLE2 in identical twins with autistic features.	Okumura A, Yamamoto T, Miyajima M, Shimojima K, Kondo S, Abe S, Ikeno M, Shimizu T.	Pediatr Neurol 51: 730-3, 2014.	2014	国外
Whole exome sequencing reveals recurrent mutations in BRCA2 and FAT genes in acinar cell carcinomas of the pancreas.	Furukawa T, Sakamoto H, Takeuchi S, Ameri M, Kuboki Y, Yamamoto T, Hatori T, Yamamoto M, Sugiyama M, Ohike N, Yamaguchi H, Shimizu M, Shibata N, Shimizu K, Shiratori K.	Scientific Reports [in press]	2014	国外
Network-based gene expression analysis of vascular wall of juvenile Moyamoya disease.	Okami N, Aihara Y, Akagawa H, Yamaguchi K, Kawashima A, Yamamoto T, Okada Y.	Childs Nerv Syst [Epub ahead of print]	2014	国外
Single nucleotide variations in CLCN6 identified in patients with benign partial	Yamamoto T, Shimojima K, Sangu N, Komoike Y, Ishii A, Abe S, Yamashita	Plos One [in press]	2014	国外

epilepsies in infancy and/or febrile seizures.	S, Imai K, Kubota T, Fukasawa T, Okanishi T, Enoki H, Tanabe T, Saito A, Furukawa T, Shimizu T, Milligan CJ, Petrou S, Heron SE, Dibbens LM, Hirose S, Okumura A.			
An association of 19p13.2 microdeletions with Malan syndrome and Chiari malformation.	Shimojima K, Okamoto N, Tamasaki A, Sangu N, Shimada S, Yamamoto T.	Am J Med Genet A [in press]	2014	国外
Epilepsy in 1p36 deletion syndrome is not associated with deletion size.	Yamamoto T, Shimada S, Shimojima K, Ikeda H, Oguni K.	J Pediatr Epilepsy [in press]	2014	国外
Xq28 duplications and epilepsy: Influence of the combinatory duplication of MECP2 and GDI1.	Yamamoto T, Shimada S, Shimojima K, Eto K, Yoshitomi S, Yanagihara K, Imai K, Oguni H, Okamoto N.	J Pediatr Epilepsy [in press]	2014	国外
Epilepsies in children with 2q24.3 deletion/duplication.	Okumura A, Yamamoto T, Kurahashi H, Takasu M.	J Pediatr Epilepsy [in press]	2014	国外
Epilepsy and other symptoms associated with chromosome 9q34.11 microdeletion.	Akiyama T, Yamamoto T.	J Pediatr Epilepsy [in press]	2014	国外
16p11.2 microdeletion/ microduplication syndrome and benign infantile epilepsy.	Tsurusawa R, Ihara Y, Ogawa A, Yamamoto T.	J Pediatr Epilepsy [in press]	2014	国外
iPS 細胞（幹細胞）を用いる医療の近未来	山本俊至，下島圭子	遺伝子医学 MOOK 別冊「今さら聞けない『遺伝医学』」. pp173-181，メディカルドゥ，大阪，2014.	2014	国内
1p36 欠失症候群	山本俊至	今日の小児治療指針，水口雅，ら 編．医学書院，東京 [in press]	2014	国内
Rett 症候群	山本俊至	今日の小児治療指針，水口雅，ら 編．医学書院，東京 [in press]	2014	国内

先天性疾患の疫学および遺伝的基礎	山本俊至	ネルソン小児科学第19版（翻訳），エルゼビアジャパン [in press]	2014	国内
ダウン症候群・染色体異常	山本俊至	こどもの神経の診かた，新島新一，山内秀雄，山本仁編．医学書院，東京 [in press]	2014	国内
マイクロアレイ染色体検査概論	山本俊至	小児内科47巻増刊号　病態生理2 [in press]	2014	国内
アレイCGH法によるてんかんの分子診断	山本俊至	医学のあゆみ [in press]	2014	国内

研究成果の刊行物・別刷（抜粋）

Original Research

Attenuation of endoplasmic reticulum stress in Pelizaeus-Merzbacher disease by an anti-malaria drug, chloroquine

Toshifumi Morimura[1,2,3], Yurika Numata[1,4], Shoko Nakamura[1], Eriko Hirano[1], Leo Gotoh[1], Yu-ich Goto[1], Makoto Urushitani[2,*] and Ken Inoue[1]

[1]Department of Mental Retardation and Birth Defect Research, National Institute of Neuroscience, National Center of Neurology and Psychiatry (NCNP), 4-1-1 Ogawahigashi-machi, Kodaira-shi, Tokyo 187-8502, Japan; [2]Unit for Neurobiology and Therapeutics, Molecular Neuroscience Research Center, Shiga University of Medical Science, Seta-Tsukinowa-cho, Otsu, Shiga 520-2192, Japan; [3]Unit for Animal Model of Neurological Disorders, Molecular Neuroscience Research Center, Shiga University of Medical Science, Seta-Tsukinowa-cho, Otsu, Shiga 520-2192, Japan; [4]Department of Pediatrics, Graduate School of Medicine, Tohoku University, 1-1 Seiryo-cho, Aoba-ku, Sendai-shi, Miyagi 980-0872, Japan

*Present address: Department of Neurology, Kyoto University Graduate School of Medicine, 54 Shogoin-Kawahara-cho, Sakyo-ku, Kyoto 606-8507, Japan

Corresponding authors: Toshifumi Morimura. Emails: morimura@belle.shiga-med.ac.jp; Ken Inoue. Email: kinoue@ncnp.go.jp

Abstract

Pelizaeus-Merzbacher disease (PMD) is a hypomyelinating disorder caused by the duplication and missense mutations of the proteolipid protein 1 (*PLP1*) gene. PLP1 missense proteins accumulate in the endoplasmic reticulum (ER) of premature oligodendrocytes and induce severe ER stress followed by apoptosis of the cells. Here, we demonstrate that an anti-malaria drug, chloroquine, decreases the amount of an ER-resident mutant PLP1 containing an alanine-243 to valine (A243V) substitution, which induces severe PMD in human. By preventing mutant PLP1 translation through enhancing the phosphorylation of eukaryotic initiation factor 2 alpha, chloroquine ameliorated the ER stress induced by the mutant protein in HeLa cells. Chroloquine also attenuated ER stress in the primary oligodendrocytes obtained from myelin synthesis deficit (*msd*) mice, which carry the same *PLP1* mutation. In the spinal cords of *msd* mice, chloroquine inhibited ER stress and upregulated the expression of marker genes of mature oligodendrocytes. Chloroquine-mediated attenuation of ER stress was observed in HeLa cells treated with tunicamycin, an N-glycosylation inhibitor, but not with thapsigargin, a sarco/ER Ca^{2+}ATPase inhibitor, which confirms its efficacy against ER stress caused by nascent proteins. These findings indicate that chloroquine is an ER stress attenuator with potential use in treating PMD and possibly other ER stress-related diseases.

Keywords: PMD, PLP, ER stress, UPR, chloroquine, treatment

***Experimental Biology and Medicine* 2014; 239: 489–501. DOI: 10.1177/1535370213520108**

Introduction

In the central nervous system, oligodendrocytes form the myelin sheath by wrapping axons with multiple layers of their plasma membrane; this enables rapid impulse conduction along the axons and prevents neuronal death.[1–3] Compact myelin, the lipid-rich major component of the myelin sheath, has a unique composition with more than 70% lipid by dry weight, and 80% of its protein mass consists of just two proteins, myelin basic protein (MBP), and proteolipid protein 1 (PLP1).[1] Although *shiverer*[4] (*Mbp*-deficient) mice develop a severe hypomyelinating disorder in the central and peripheral nervous systems and a corresponding shortened lifespan, the phenotypes of *Plp1*-knockout mice[5] and *PLP1*-null humans[6,7] display extremely mild myelin defects with almost normal lifespan.

While complete deficiency of *PLP1* only causes modest neurological symptoms, duplication and missense mutations of the *PLP1* gene result in a severe hypomyelinating disorder, Pelizaeus-Merzbacher disease (PMD). PMD is an X-linked recessive leukodystrophy characterized by failure of myelination in the central nervous system.[8,9] Duplication of the *PLP1* gene accounts for 60–70% of PMD cases,[10,11] but it remains unclear why an excess amount of PLP1 induces severe hypomyelination. In contrast, missense mutations of

ISSN: 1535-3702

PLP1 are known to inhibit export of the proteins from the endoplasmic reticulum (ER) and induce wide-range ER stress. This results in a broad clinical spectrum, ranging from severe PMD to milder spastic paraplegia type 2.[8,12,13] Accumulation of unfolded/misfolded proteins such as PLP1 mutants in the ER activates the unfolded protein response (UPR) by the three ER stress sensors: (1) inositol-requiring kinase 1 (IRE1, also known as ER-to-nucleus signaling 1); (2) protein kinase-like ER kinase (PERK, also known as eukaryotic translation initiation factor 2 alpha kinase 3); and (3) activating transcription factor 6 (ATF6). These sensors maintain ER homeostasis via three mechanisms: (1) an increase in ER folding capacity by enhancing transcription/translation of ER chaperones; (2) retrotranslocation of unfolded/misfolded proteins from the ER to the cytosol, followed by ER-associated degradation (ERAD) that is dependent on the ubiquitin-proteasome system; and (3) inhibition of protein synthesis, which prevents ER entry of secretory and membrane proteins.[14] When unfolded/misfolded protein accumulation in the ER exceeds the capacity of the repair system, it induces ER stress and subsequent apoptosis. The apoptotic events are the primary cause of ER stress-related diseases, including PMD. Thus, decreasing the amount of unfolded/misfolded proteins in the ER may be therapeutic in ER stress diseases. In the present study, we investigated a possible therapy against ER stress-related diseases by using a mutant PLP1 containing an alanine-243 to valine (A243V) substitution, which models severe PMD in mice (known as *myelin synthesis deficit* (*msd*) mice)[15] as well as causes human PMD.[16] We found that chloroquine (CQ), a well-known anti-malaria medicine,[17] attenuates ER stress *in vitro* and *in vivo* by inhibiting translation of the mutant protein.

Material and methods

Mice

Msd mice, which carry the spontaneous A243V mutation in the *Plp1* gene,[15] were a kind gift from Dr W.B. Macklin (Cleveland Clinic Foundation). The mice were maintained on a B6C3F1/J background and housed on a 12-h light/dark cycle in a specific pathogen-free environment. To investigate the effects of CQ *in vivo*, postnatal day 14 (P14) mice were intraperitoneally injected with CQ (0.5 mg/mL phosphate-buffered saline [PBS], 10 μL/g body weight) or PBS alone, and immunoblot (IB), quantitative polymerase chain reaction (qPCR), and immunohistochemistry were performed after 6 h. The injected dose of CQ is commonly used to treat malarial infection in mice. Mice were handled in accordance with institutional guidelines of the animal care committee of the National Institute of Neuroscience, National Center of Neurology and Psychiatry.

Plasmids and reagents

The expression vectors used here have been described previously.[13] In brief, the C-terminals of PLP1 wild-type (wtPLP1) and A243V mutant (msdPLP1) genes were fused in frame with FLAG epitope sequence and the fusion genes were driven under a hybrid promoter consisting of the chicken β-actin promoter and cytomegalovirus early enhancer. The following reagents were purchased: chloroquine, thapsigargin, MG-132, leupeptin, pepstatin A, bafilomycin A1 (all from Sigma-Aldrich), lactacystin (Biomol), and tunicamycin (Merck). The following primary antibodies were used for immunoblotting: mouse anti-FLAG (M2; Sigma-Aldrich), mouse anti-β actin (MAB1501; Millipore), mouse anti-ubiquitin (P4D1; Santa Cruz Biotechnology), and rabbit anti-pT981 PERK (sc-32577; Santa Cruz Biotechnology), rabbit anti-PERK (ac-13073; Santa Cruz Biotechnology), rabbit anti-pS51 eIF2α (#3597; Cell Signaling), rabbit anti-eIF2α (#9722; Cell Signaling), rabbit anti-PLP1 (a kind gift from Dr M. Itoh, NCNP), and mouse anti-MBP (SMI99; Covance). Horseradish peroxidase-conjugated secondary antibodies were purchased from GE Healthcare.

Cell culture, transfection, immunoblotting, and immunoprecipitation

HeLa cells were maintained in Dulbecco's modified Eagle medium (Sigma-Aldrich) containing 10% fetal bovine serum and antibiotics. For immunoblotting, HeLa cells were plated onto 6-well plates and transfected with the expression vectors by using TransIt Lt1 (Mirus) according to the manufacturer's instructions. Twenty-four hours later, cells were treated with indicated reagents and lysed with TNE lysis buffer (50 mM Tris [pH8.0], 2 mM EDTA, 150 mM NaCl, 0.1% SDS, 1% TritonX-100, and appropriate protease and phosphatase inhibitors). Lysates were immunoprecipitated and immunoblotted as described previously.[18]

Mixed glial culture

Preparation of mixed glial cultures and induction of oligodendrocyte differentiation were performed as previously described.[13] On the fourth day of differentiation, the cells were treated with 100 or 200 μM of CQ for 6 h, followed by collection of protein and RNA samples.

Pulse-chase experiment

To analyze the amount of translated msdPLP1-FLAG, transfected cells were pulsed with 20 μCi/mL of ^{35}S-methionine/cysteine in the presence of CQ for 30 min. To analyze ERAD capacity, the cells were radiolabeled in the absence of CQ for 30 min, washed with culture medium three times, and then cultured for additional 3 and 6 h in the presence of 100 μM CQ. Subsequently, lysates were subjected to immunoprecipitation (IP) with M2-coated agarose (Sigma-Aldrich) followed by autoradiography using an image analyzer (BAS2000; Fuji).

Terminal deoxynucleotidyl transferase dUTP nick end labeling

P14 mice were perfused with 4% paraformaldehyde, and their spinal cords were subjected to terminal deoxynucleotidyl transferase dUTP nick end labeling (TUNEL) analysis

by using ApopTag kit (Millipore) following anti-MBP and anti-PLP1 immunohistochemistry.

qPCR

The total RNA samples from the transfected cells and P14 spinal cords were prepared using an RNeasy Protect Mini Kit (Qiagen) and converted to cDNA via Superscript III reverse transcriptase with an oligo-dT primer (Invitrogen). The levels of mRNAs for C/EBP homologous protein (*CHOP*), Glucose-regulated protein of 78 KDa (*GRP78*), *PLP1*, *MBP*, and glyceraldehyde 3-phosphate dehydrogenase (*GAPDH*) in the synthesized cDNAs were analyzed with pre-designed TaqMan probes (Applied Biosystems) and a thermal cycler (7900HT, Applied Biosystems). *GAPDH* was used as the endogenous control, and the relative expression levels of the transcripts were calculated by the ΔΔCT method according to the manufacturer's protocol. The pre-designed TaqMan probes used in this study were human *GAPDH*, Hs99999905; human *CHOP*, Hs00358796; human *GRP78*, Hs99999174; mouse *Gapdh*, Mm99999915; mouse *Plp1*, Mm01297210; mouse *Mbp*, Mm01266402; mouse *Chop*, Mm00492097; mouse *Grp78*, Mm00517691; and mouse *Oligo2*, Mm01210556.

Analysis of mRNA splicing of human and mouse XBP1

The mRNAs of human and mouse X-box binding protein 1 (*XBP1*) were amplified by using following primer sets: human *XBP1*, 5′-ACAGCGCTTGGGGATGGATG-3′ and 5′-TGACTGGGTCCAAGTTGTCC-3′; mouse *Xbp1*, 5′-TTACGGGAGAAAACTCACGGC-3′ and 5′-GGGTCCAA CTTGTCCAGAATGC-3′. The mRNAs of human and mouse *GAPDH* were amplified using the same primer set, 5′-ACCACAGTCCATGCCATCAC-3′ and 5′-TCCACCAC CCTGTTGCTGTA-3′. The PCR products of the *XBP1* and *GAPDH* were analyzed by 3% and 1.5% agarose gel electrophoresis, respectively.

Statistical analysis

All data from cellular experiments using HeLa cells and oligodendrocytes, except data shown in Figure 2(d) and (e), were obtained from three independent experiments performed on three different days. The relative expression levels of proteins and RNAs were normalized to control levels (100%), and results were expressed as fold changes. Student's *t*-test and analysis of variance (ANOVA) were used for statistical analysis of differences between two groups and more than two groups, respectively.

Results

Reduction of the amount of msdPLP1 in the presence of CQ

First, to compare the amounts of the mutant PLP1 in the presence of proteasome or lysosome inhibitors, HeLa cells that had been transiently transfected with the FLAG-tagged msdPLP1 (msdPLP1-FLAG) gene were treated with the respective inhibitors for 6 h and whole cell extracts were immunoblotted (Figure 1a). As with newly synthesized protein,[12,19] the amount of mutant protein was increased in the presence of proteasome inhibitors (lanes2–3, Figure 1a). This confirmed that msdPLP1 is degraded via the ERAD pathway.

ER stress proteins have been shown to be eliminated not only by ERAD but also by the lysosome-dependent bulk protein degradation pathway, i.e. autophagy.[20,21] Indeed, bafilomycin A1 (lane 5, $P = 0.0028$, Figure 1a), which inhibits lysosomal function through alkalization by inhibiting vacuolar type H^+-ATPase, increased the amount of the mutant protein. However, lysosomal protease inhibitors leupeptin and pepstatin A (Leu/PepA, lane 4, Figure 1a) failed to increase mutant PLP1 levels. On the other hand, the amount of mutant protein was significantly lower in the presence of another lysosome inhibitor, CQ (lane 6, Figure 1a). A time course study showed that after incubation for 6 h, CQ significantly reduced the amount of mutant protein (Figure 1b). The total amount of msdPLP1-FLAG was slightly higher when incubated with a lower concentration of CQ (10 μM), but was significantly less at higher concentrations (75–100 μM, Figure 1c). These results suggest that CQ decreases the amount of msdPLP1-FLAG in a manner that is independent of lysosomal inhibition. We hypothesized that CQ may instead enhance ERAD of msdPLP1-FLAG, and CQ would further increase the amount of ubiquitinated msdPLP1-FLAG above that created through another proteasome inhibitor. However, CQ did not increase ubiquitinated msdPLP1-FLAG in the presence (lanes 4 and 5, Figure 1d) or absence (lanes 2 and 3, Figure 1d) of MG-132. Furthermore, CQ did not alter the half-life of msdPLP1-FLAG (Figure 1e), indicating that CQ decreases the amount of msdPLP1-FLAG without increasing ERAD capacity.

CQ phosphorylates eIF2α and inhibits translation

Next, we biochemically analyzed the signaling pathway of ER stress in transfected HeLa cells treated with CQ (Figure 2a). We observed that CQ induced eukaryotic initiation factor 2 alpha (eIF2α) phosphorylation but not the phosphorylation and activation of an upstream kinase, PERK, one of the ER stress sensors.[22] Moreover, eIF2α phosphorylation gradually increased in the cells transfected with either the msdPLP1-FLAG gene or empty vector (Figures 2(a) and (b)). It is noteworthy that CQ preferentially induced eIF2α phosphorylation in the cells transfected with the msdPLP1 gene but not as much in the control cells at each time point in three independent experiments.

Since phosphorylation of eIF2α inhibits general translation,[23] we performed a pulse-chase experiment with ^{35}S-methionine/cysteine in the presence of CQ in HeLa cells. CQ significantly inhibited msdPLP1-FLAG translation during the 30-min incubation at 200 μM (Figure 2c, gray column), but incubation at 100 μM did not reach significance ($P = 0.1034$, Figure 2(c), black column). Furthermore, CQ also inhibited the production of exogenous wild type PLP1 in HeLa cells (Figure 2d) and endogenous PLP1 in mature oligodendrocytes in mixed glial cultures (Figure 2e). CQ inhibits translation in retinal pigment epithelial cells at a much higher concentration.[24] Taken together,

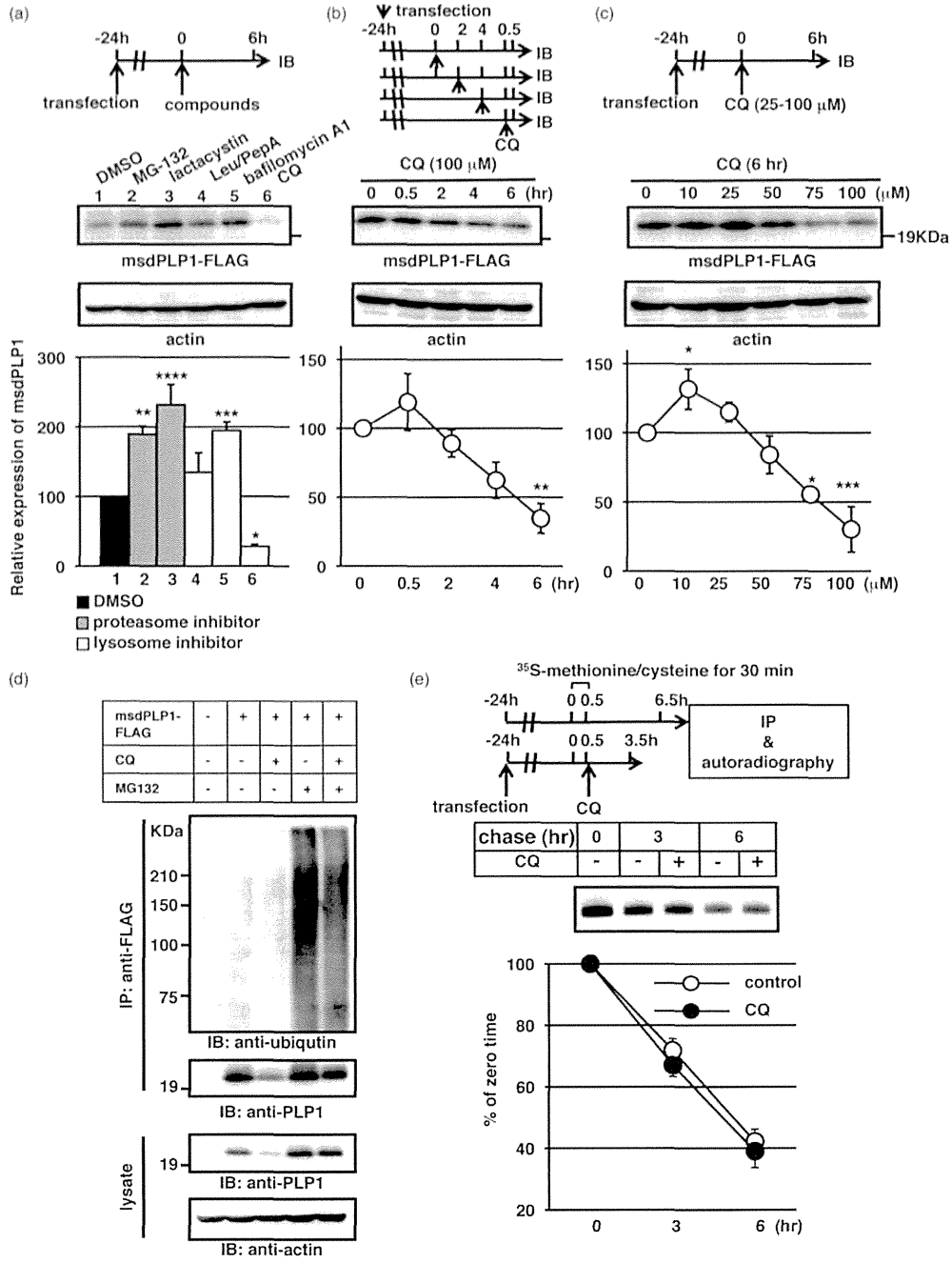

Figure 1 Expression of msdPLP1-FLAG in HeLa cells in the presence of lysosome or proteasome inhibitors. (a) Effects of protease inhibitors on the amount of msdPLP1-FLAG. Top: Schematic diagram of the experiment. HeLa cells were transfected with the msdPLP1-FLAG gene, incubated for 24 h, and treated with the indicated compounds for 6 h. Middle: Protein samples were then subjected to immunoblotting. Bottom: Immunoblot results with corresponding lane numbers. For all immunoblots, densitometric analysis was carried out to measure the amounts of msdPLP1-FLAG and β-actin, and the relative expression level of PLP1 (FLAG/β-actin) is shown as fold change by comparing with control cells (lane1, 100%). (b) Time course of msdPLP1-FLAG levels. Top: Schematic diagram of the experiment. Transfected cells were incubated for 30 h. During the last 0.5, 2, 4, and 6 h, the cells were reacted with 100 μM CQ. Middle: Cells were then immunoblotted with anti-FLAG and anti-actin antibodies. Bottom: The relative expression levels. (c) Dose-dependent effects of CQ on msdPLP1-FLAG levels. Top: Schematic diagram of the experiment. Transfected cells were incubated over 30 h. During the last 6 h, the cells were treated with 25, 50, 75, and 100 μM CQ. Middle: Immunoblot with anti-FLAG and anti-actin antibodies. Bottom: The relative expression levels. (d) Ubiquitinated msdPLP1-FLAG in the presence of CQ and/or MG-132. The experiment was performed as in Figure 1(a), and precipitated samples and cell lysates were immunoblotted with anti-ubiquitin and anti-PLP1 antibodies. (e) Stability of msdPLP1-FLAG in the presence of CQ. Top: Schematic diagram of the experiment. Transfected cells were radiolabeled for 30 min in the absence of CQ, further cultured for 3 h and 6 h in the absence or presence of CQ, and cell extracts were immunoprecipitated with the anti-FLAG antibody followed by autoradiography (middle and bottom). All graphs in Figure 1 are shown with means ± SEM ($n = 3$). Leu: leupeptin; PepA: pepstatin A; CQ: chloroquine. *$P < 0.05$; **$P < 0.005$; ***$P < 0.001$; ****$P < 0.0005$

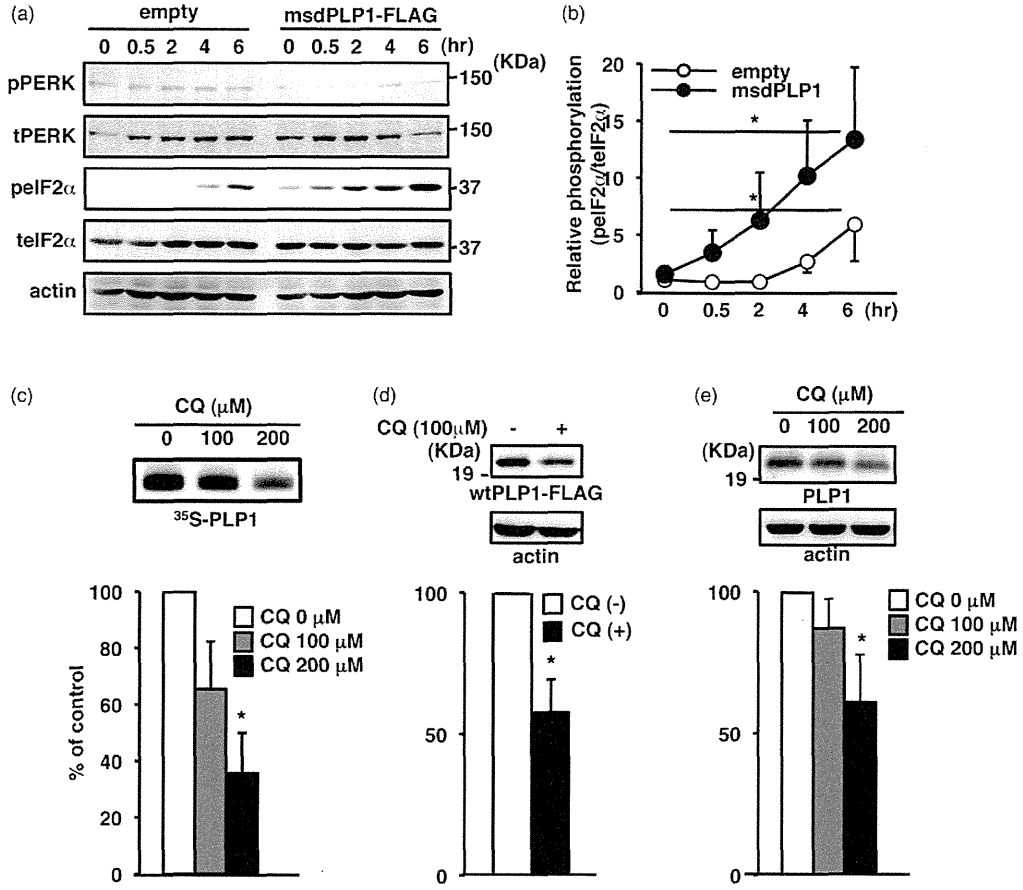

Figure 2 CQ Inhibits translation through the activation of eIF2α. (a, b) Phosphorylation of eIF2α in the presence of CQ. Transfected cells were treated or not treated with 100 μM CQ for 0.5–6 h, and cell lysates were immunoblotted with indicated antibodies (a). The experiment was performed as in Figure 1(b). The blots were densitometrically analyzed to measure the relative phosphorylation level of eIF2α between control (open circles) and msdPLP1-FLAG-transfected cells (closed circles), shown as fold increment as compared to the mean of CQ-untreated control cells (100%) (b). (c) Efficacy of translation of msdPLP1-FLAG in the presence of CQ. Transfected cells were radiolabeled for 30 min in the presence of CQ, and cell lysates were subjected to autoradiography (top) followed by quantitative analysis (bottom) as in Figure 1(e). (d) Expression of wild-type (wt)PLP1-FLAG in the presence of CQ. HeLa cells expressing wtPLP1-FLAG were treated with CQ for 6 h. Cell lysates were then immunoblotted with the indicated antibodies (top) and densitometrically analyzed (bottom). (e) Expression of endogenous PLP1 in the presence of CQ. Mixed glial cultures were treated with CQ for 6 h and cell lysates were then immunoblotted with anti-PLP1 and anti-β-actin antibodies. All graphs in Figure 2 are shown as means ± SEM ($n = 3$). *$P < 0.05$

these results suggest that CQ inhibits translation of the mutant protein by inducing phosphorylation of eIF2α.

CQ attenuates msdPLP1-induced ER stress in vitro

To investigate whether CQ regulates ER stress caused by msdPLP1-FLAG, we collected RNA samples from transfected cells and amplified *XBP1* mRNA, which is spliced by IRE1 to produce mature functional XBP1 in response to ER stress[25–27] (Figure 3a). CQ by itself did not alter the splicing of *XBP1* mRNA in the control cells. However, transfection of the msdPLP1-FLAG gene significantly increased the proportion of spliced *XBP1* mRNA. When the transfected cells were treated with CQ, the proportion of spliced *XBP1* mRNA significantly decreased.

We also performed qPCR using *CHOP* (also known as DNA damage-inducible transcript 3) mRNA and *GRP78* (also known as 70 KDa heat shock protein) mRNA, both of which are upregulated by ER stress.[14] Unexpectedly, expression of *CHOP* mRNA was significantly elevated (>2-fold) by CQ in control cells, and we were unable to determine whether CQ inhibits msdPLP1-FLAG-induced *CHOP* expression (Figure 3b). In contrast, expression of the *GRP78* mRNA was unaltered by CQ in control cells, but was elevated 2-fold by msdPLP1-FLAG. This induction was significantly decreased in the presence of CQ (Figure 3c). Similarly, CQ significantly decreased the expression of *Grp78* in cultured oligodendrocytes from *msd* mice, whereas it greatly upregulated that of *Chop* in the cells from both wild-type and mutant animals (Figure 3(d) and (e)).

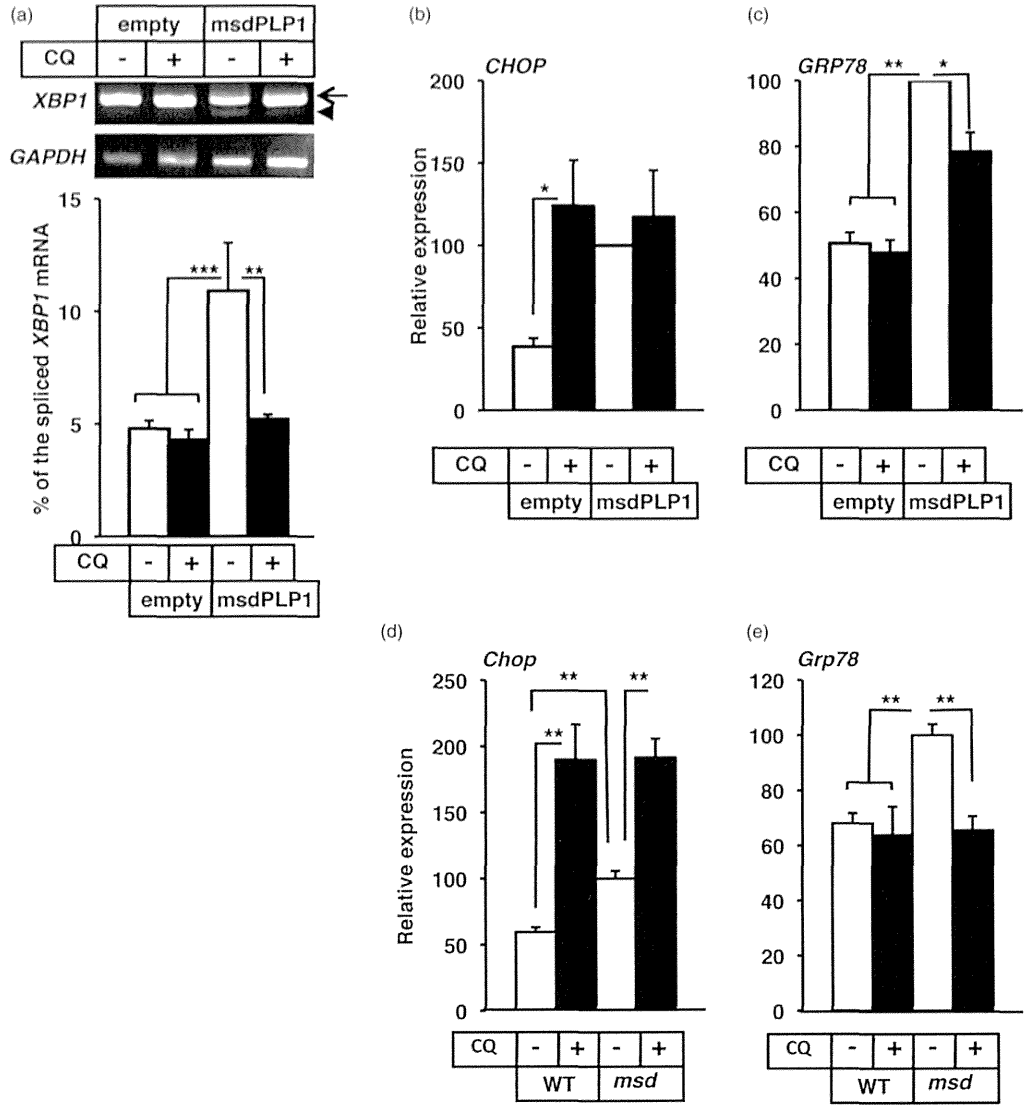

Figure 3 UPR in msdPLP1-expressing HeLa cells and oligodendrocytes in the presence of CQ. (a) Splicing of *XBP1* mRNA in HeLa cells transfected with the msdPLP1-FLAG gene. *XBP1* mRNA was amplified from RNA samples of the transfected cells treated with CQ for 4 h, analyzed by 3% agarose gel electrophoresis, and the percentage of spliced *XBP1* mRNA was calculated. The arrow and arrowhead indicate the bands of the unspliced and spliced *XBP1* mRNA, respectively. (b, c) Relative expression of *CHOP* mRNA (b) and *GRP78* mRNA (c) in HeLa cells expressing msdPLP1-FLAG. RNA samples were subjected to qPCR in order to measure relative expression of the mRNAs. *GAPDH* mRNA was used as the endogenous control, and results are shown as fold change by comparing with the expression level in CQ-untreated, msdPLP1-expressing HeLa cells. (d, e) Relative expression of *Chop* (d) and *Grp78* (e) mRNAs in mixed glial cultures from wild-type and *msd* mice. After induction of oligodendrocyte differentiation, cells were treated with CQ for 6 h, and their RNA samples were subjected to qPCR. *GAPDH* mRNA was used as the endogenous control. Results are shown as fold change by comparing with the expression level in CQ-untreated cells obtained from *msd* mice. All graphs in Figure 3 are shown as means ± SEM ($n = 3$). $^{*}P < 0.05$; $^{**}P < 0.01$; $^{***}P < 0.005$; $^{****}P < 0.001$

CHOP mRNA expression is enhanced not only by the activation of the IRE1-XBP1 branch of UPR, but also by other signaling pathways, including the eIF2α phosphorylation pathway.[28] Thus, the opposite responses of *CHOP* and *GRP78* mRNA may be attributed to eIF2α phosphorylation. Taken together, these results suggest that CQ attenuates ER stress caused by msdPLP1-FLAG by inhibiting translation.

UPR in the spinal cords of msd mice treated with CQ

To investigate the effect of CQ on ER stress *in vivo*, we intraperitoneally injected CQ into *msd* male mice at P14, when the expression of *Plp1* peaks in the spinal cords of the mutant mice.[29] The spinal cords of *msd* mice had sparse MBP^{+} myelin fibers, decreased numbers of PLP1^{+} cells, and exhibited increased apoptosis in the MBP-positive regions (Figure 4a). Protein and mRNA levels of both MBP

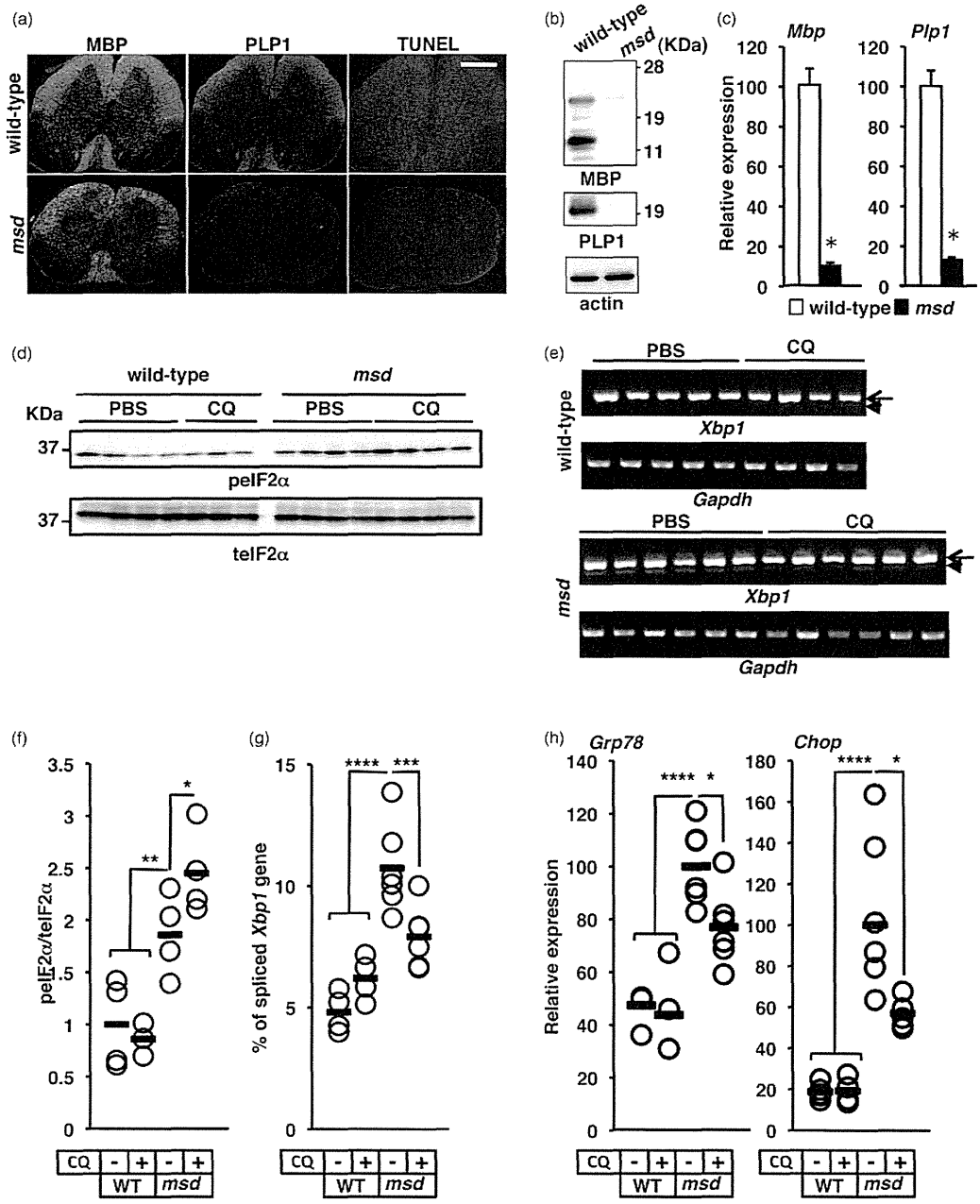

Figure 4 Attenuation of ER stress in the spinal cords of P14 *msd* mice treated with CQ. (a–c) Phenotypic analysis of the spinal cords of P14 *msd* mice. (a) Histological analysis. The spinal cord sections of wild-type mice (top) and *msd* mice (bottom) were immunolabeled for MBP (left), PLP1 (center), and apoptotic cells (right). Scale bar = 500 μm. (b) Immunoblot analysis of MBP and PLP1. Protein samples of the spinal cords were immunoblotted with antibodies against MBP, PLP1, and β-actin. (c) Relative expression of the *Mbp* mRNA (left) and *Plp1* mRNAs (right). Total RNA samples from wild-type (open column, $n = 5$) and *msd* (closed column, $n = 6$) mice were subjected to qPCR analysis to measure the expression levels of the mature oligodendrocyte markers *Mbp* and *Plp1*. *Gapdh* mRNA was used as the endogenous control. Graphs indicate means ± SEM (wild-type, $n = 5$; *msd*, $n = 6$). *$P < 0.001$. (d, f) Phosphorylation of eIF2α in the spinal cords of P14 wild-type and *msd* mice treated with CQ. Protein samples from wild-type and *msd* mice injected or not injected with CQ were immunoblotted with indicated antibodies (d), and the blots were densitometrically analyzed to measure the relative phosphorylation of eIF2α, as in Figure 2(b). Open circles and horizontal bars indicate individual relative phosphorylation levels and means, respectively (f). (e, g) Splicing of *Xbp1* in the spinal cords of P14 wild-type and *msd* mice treated with CQ. The *Xbp1* mRNA was analyzed as described previously as in (Figure 3a). The arrow and arrowhead indicate the bands of the unspliced and spliced *Xbp1* mRNA, respectively (e). The percentage of spliced *Xbp1* mRNA was calculated as in Figure 3(a). Open circles and horizontal bars indicate individual splicing levels and means, respectively (g). (h, i) Relative expression of *Grp78* (h) and *Chop* (i) mRNAs in the spinal cords of P14 wild-type *msd* mice treated with CQ. Total RNA samples from the spinal cords of wild-type and *msd* mice injected with CQ or PBS alone were subjected to qPCR analysis to measure the relative expression levels of ER stress markers *Grp78* and *Chop*, with *Gapdh* used as the endogenous control. Sample sizes were as follow: wild-type/PBS, $n = 5$; wild-type/CQ, $n = 4$; msd/PBS, $n = 6$; and msd/CQ, $n = 6$. Open circles and horizontal bars indicate individual expression levels and means, respectively (g). *$P < 0.05$; **$P < 0.01$; ***$P < 0.005$; ****$P < 0.001$

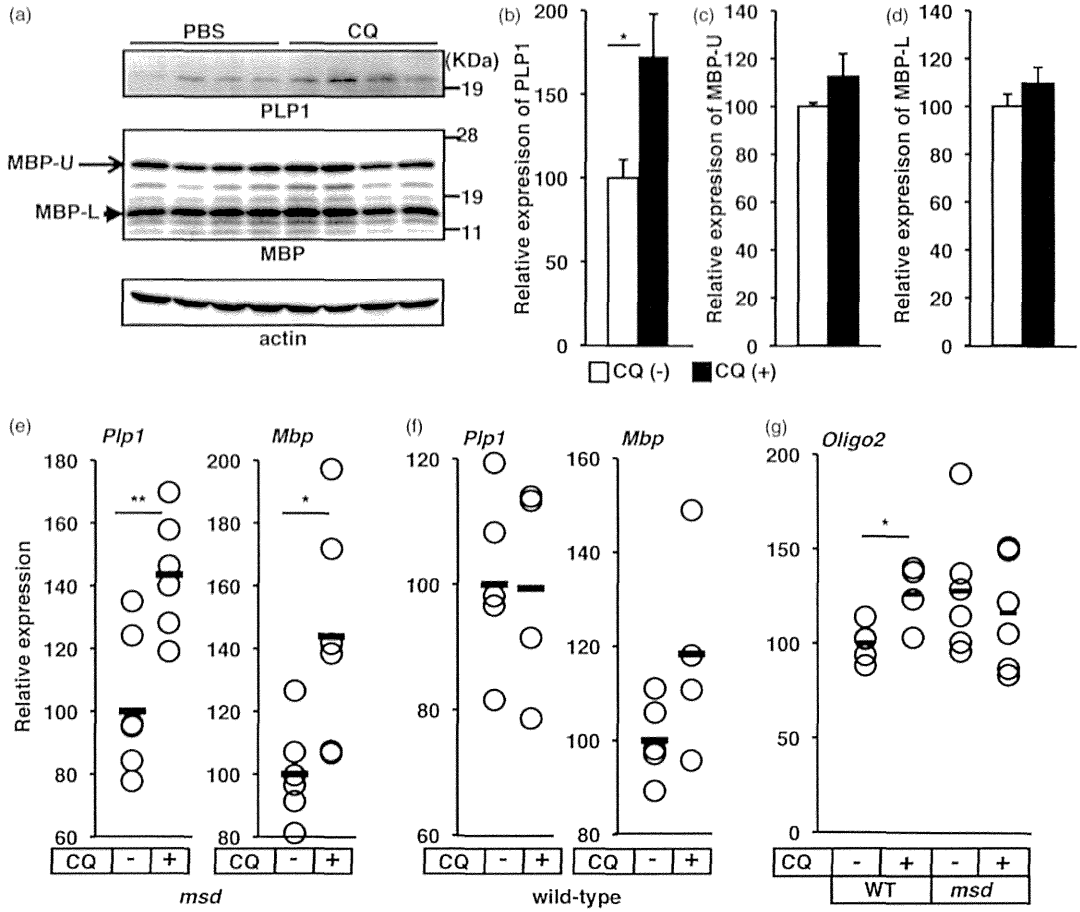

Figure 5 Expression of mature oligodendrocyte markers in the spinal cords of P14 *msd* mice injected with CQ. (a–d) Amounts of PLP1 and MBP. Protein samples of *msd* mice were immunoblotted with antibodies against PLP1, MBP, and β-actin (a), and the blots were densitometrically analyzed to measure the relative expression levels of PLP1 (b), MBP-U (c), and MBP-L (d). Results are shown as means ± SEM. (e, f) Relative expression of *Plp1* and *Mbp* mRNAs in *msd* (e) and wild-type mice (f) treated with CQ. (g) Relative expression of *Oligo2* mRNA. Total RNA samples were treated as described previously (Figure 4h/i) to measure relative expression levels of the mature oligodendrocyte markers *Plp1* and *Mbp*, and the pan-oligo marker *Oligo2*. *Gapdh* mRNA was used as the endogenous control. Open circles and horizontal bars in (e), (f), and (g) indicate individual relative expression levels of the transcripts and means, respectively. Sample sizes were: wild-type/PBS, $n = 5$; wild-type/CQ, $n = 4$; msd/PBS, $n = 6$; msd/CQ, $n = 6$. $^{*}P < 0.05$; $^{**}P < 0.01$

and PLP1 were drastically decreased, possibly because of the premature death of oligodendrocytes (Figure 4(b) and (c)).

First, we analyzed the phosphorylation of eIF2α in the wild type and *msd* spinal cords (Figures 4(d) and (f)). Basal eIF2α phosphorylation was significantly higher in the *msd* mice. Although CQ did not increase eIF2α phosphorylation in the wild-type mice, it significantly increased phosphorylation in the *msd* mice. The selective increase in eIF2α phosphorylation by CQ in the *msd* mice was similar to the results obtained in the transfected HeLa cells (Figure 2(a) and (b)). Because CQ crosses the blood-brain barrier and enters the central nervous system,[30] these results likely reflect a direct action by CQ. The splicing of *Xbp1* mRNA and expression of ER stress markers, *Grp78* and *Chop*, were significantly decreased by CQ in the *msd* mice (Figure 4(e) and (g), (i)). These results indicate that CQ inhibits translation and attenuates ER stress caused by the mutant PLP1 *in vivo*.

Upregulation of mature oligodendrocyte markers in msd mice injected with CQ

We then probed the same protein samples with an anti-PLP1 antibody. Despite the improvement of the ER stress signs described above, and contrary to what we observed in HeLa cells (Figure 1), CQ significantly increased the amount of PLP1 in *msd* mice (Figure 5(a) and (b)). Furthermore, *Plp1* mRNA expression was significantly higher in the mutant spinal cords treated with CQ than in those treated with PBS alone (Figure 5e, left). PLP1 is a marker of mature oligodendrocytes; its expression appeared to be significantly reduced in *msd* mice because

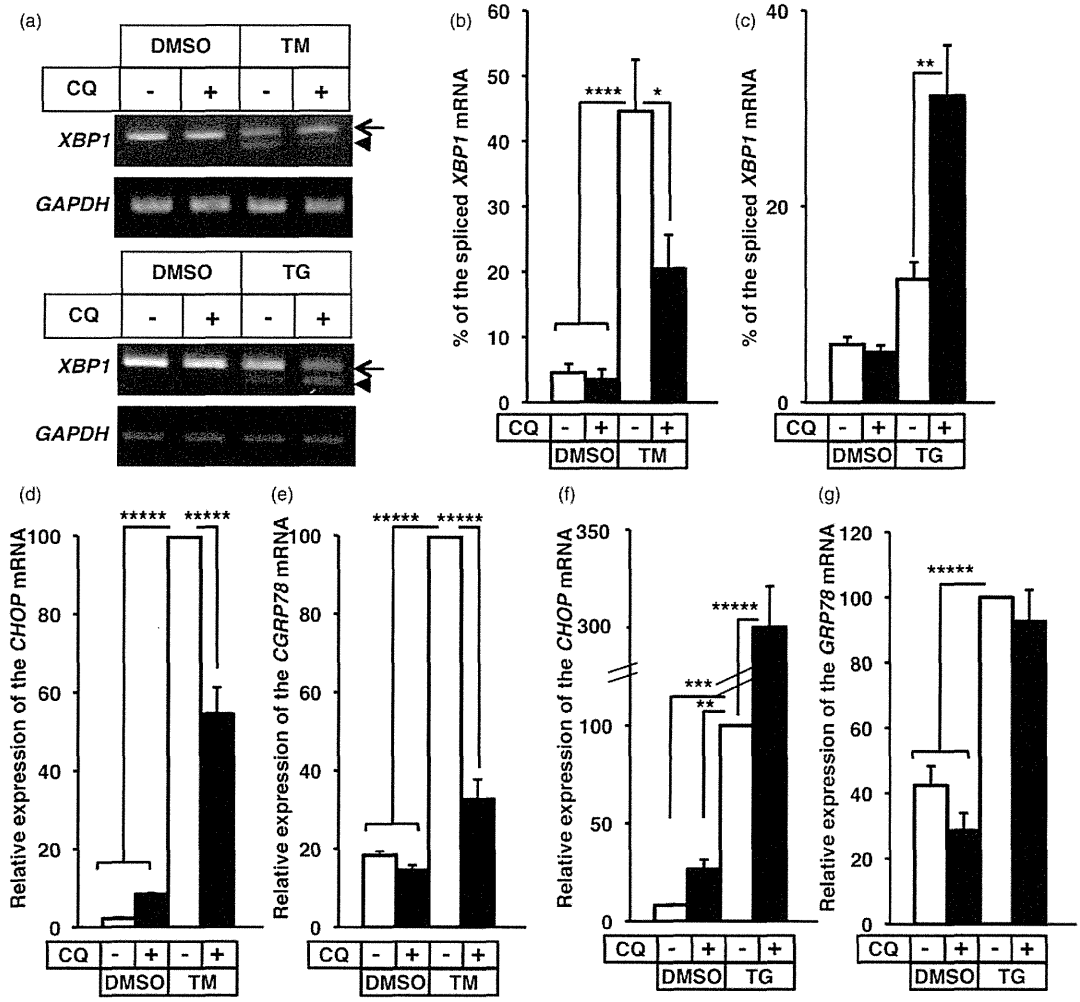

Figure 6 UPR caused by tunicamycin or thapsigargin in the presence of CQ. (a–c) Splicing of *XBP1* mRNA in HeLa cells treated with CQ, tunicamycin (TM), or thapsigargin (TG). HeLa cells were treated with 2 μM TM or 0.25μM TG together with 100 μM CQ for 4 h, and *XBP1* mRNA was amplified and analyzed by 3% agarose gel electrophoresis. The arrow and arrowhead indicate the bands of the unspliced and spliced *XBP1* mRNA, respectively (a). Bands were densitometrically analyzed to measure the relative amount of spliced *XBP1* mRNA in HeLa cells treated with TM (b) or TG (c). (d–g) Relative expression of *CHOP* (d and f) and *GRP78* (e and g) mRNAs in HeLa cells treated with TM (d and e) or TG (f and g) together with CQ. RNA samples were subjected to qPCR to measure the relative expression of the *CHOP* and *GRP78* mRNAs, with *GAPDH* mRNA as the endogenous control. All measurements in Figure 6 represent means ± SEM ($n = 3$). TM: tunicamycin; TG: thapsigargin; CQ: chloroquine. $^{*}P < 0.01$; $^{**}P < 0.005$; $^{***}P < 0.001$; $^{****}P < 0.0005$; $^{*****}P < 0.0001$

of the premature death of oligodendrocytes (Figure 4(a)–(c)). Thus, we measured the expression of another mature oligodendrocyte marker, *Mbp* mRNA, and its gene product. Although CQ did not increase the amounts of the major splice variants of MBP, namely MBP-U (upper, 21.5 kDa) and MBP-L (lower, 14 kDa), in *msd* mice (Figure 5(a), (c) and (d)), it significantly increased the expression of *Mbp* mRNA in these mice (Figure 5(e), right). Since the expression of MBP was much easier to detect than the expression of PLP1 in *msd* mice, despite the similar expression level of the two mRNAs (Figure 4(a) to (c)), modest increases in the expression of *Mbp* mRNA may not affect the amount of the protein. No such changes in the mRNA expression were observed in CQ-treated wild-type mice, in which oligodendrocytes are able to terminally differentiate (Figure 5f). In the wild-type mice, CQ unexpectedly increased the expression of the *Oligo2* gene, which was consistently expressed throughout the maturation of oligodendrocyte lineage cells (Figure 5g). At present, the reason for this is not known; however, hypothetically, CQ might increase the expression of *Oligo2* in terminally differentiated oligodendrocytes, which are dramatically decreased in number in *msd* mice. However, CQ did not significantly alter the gene expression in *msd* mice, indicating that CQ increased oligodendrocyte maturity markers in these mice without changing the pan-oligodendrocyte marker.

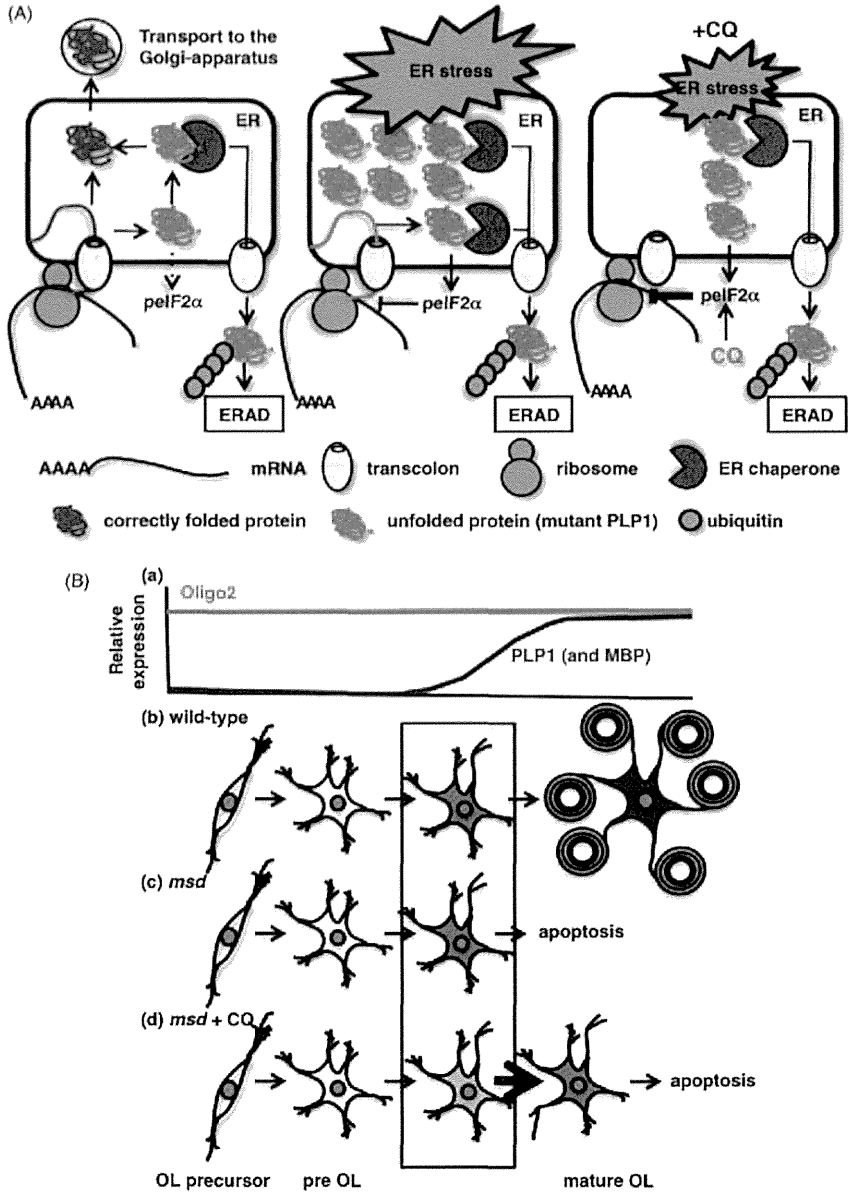

Figure 7 Model of ER stress-attenuating and oligodendrocyte-differentiating effects of CQ in *msd* mice. (A) Model of the pharmacological mechanism by which CQ attenuates ER stress. Under physiological conditions, unfolded proteins are trapped and correctly folded by ER chaperones and then transported to the Golgi apparatus (left). In ER stress-related diseases, such as PMD, unfolded mutant proteins are continuously translated, which in turn induce the unfolded protein response (UPR), including the phosphorylation of eIF2α. When the mutant protein level exceeds the repair capacity of ER chaperones, it induces ER stress, which in some case (at least in msdPLP1) is followed by apoptosis (center). CQ induces further phosphorylation of eIF2α and inhibits ER entry of the mutant proteins, thereby attenuating ER stress (right). (B) Effects of CQ on oligodendrocyte differentiation in *msd* mice. In wild-type mice, Oligo2 is expressed throughout all of the stages of oligodendrocyte differentiation, and PLP1 is expressed only in mature oligodendrocytes (a, b). In *msd* mice, oligodendrocyte precursors normally proliferate and differentiate until PLP1 is expressed. After the synthesis of myelin protein, toxic PLP1 accumulates in the ER of oligodendrocytes and induces apoptosis (c). CQ effectively reduces ER entry of the toxic protein by attenuating translation and promotes myelination and differentiation, thereby prolonging the life span of the cells (d). The square indicates the point in oligodendrocyte differentiation where myelin synthesis and the enhancement of PLP1 expression are initiated. Red and blue lines in (a) indicate relative expression levels of Oligo2 and PLP1, respectively. Blue color in (d) indicates oligodendrocytes expressing PLP1, and the blue color tones indicate the amounts of the protein. OL: oligodendrocyte. (A color version of this figure is available in the online journal)

General effects of CQ on ER stress by newly synthesized proteins

Finally, to determine whether CQ is effective against ER stress induced by newly synthesized unfolded/misfolded proteins in general, we treated HeLa cells with two well-characterized chemical ER stressors, tunicamycin, which inhibits N-glycosylation of nascent proteins, and thapsigargin, which inhibits ER Ca^{2+}ATPase. CQ significantly inhibited tunicamycin-induced splicing of *XBP1* mRNA, but accelerated thapsigargin-induced splicing (Figure 6(a) to (c)). The expression of *CHOP* was increased by CQ, as described in Figure 2, and was further upregulated by the addition of either tunicamycin or thapsigargin (Figure 6(d) and (f)). Although CQ inhibited the induction of *CHOP* by tunicamycin (Figure 6d), it increased *CHOP* expression in the presence of thapsigargin (Figure 6f). CQ also inhibited tunicamycin-induced expression of *GRP78* mRNA (Figure 6e), but it did not alter the expression level of the tunicamycin-induced chaperone gene (Figure 6g). Tunicamycin induces ER stress by altering nascent proteins, whereas thapsigargin induces ER stress by altering both newly synthesized and mature proteins. Taken together, these results confirmed that CQ effectively inhibits ER stress by blocking ER protein loading, but that it does not inhibit ER stress that results from unfolded/misfolded proteins induced after maturation.

Discussion

In this study, we reported that it might be possible to use CQ as a therapeutic agent for the treatment of the ER stress-related disorder PMD. Several compounds, such as 4-phenylbutyric acid, tauroursodeoxycholic acid,[31] and curcumin,[32,33] have been reported as effective but not completely curative against ER stress-related diseases. Therefore, significant effort has been made to identify candidate curative agents to treat ER stress.[34] Despite attenuating ER stress in experiments conducted in model systems, most of the candidate compounds identified thus far are inhibitors of signaling pathways, whose side effects entail considerable clinical challenges. Because the use of CQ in humans has been well established, its clinical use as an ER stress attenuator would offer considerable advantages with respect to safety, ethical issues, and material availability. ER stress contributes to the progression of many diseases, including neurodegenerative diseases[14]; therefore, CQ may also be therapeutic in a wide range of human diseases with similar molecular pathology.

The results of this study demonstrated that CQ effectively decreases mutant PLP1 expression by enhancing eIF2α phosphorylation, and that it attenuates ER stress in transfected HeLa cells (Figures 1–3). Consistent with these findings, we also found that CQ significantly attenuated ER stress in oligodendrocytes obtained from *msd* mice (Figure 3e) and in the spinal cords of *msd* mice (Figure 4). The CQ-mediated attenuation of ER stress *in vivo* is probably mediated by inhibiting protein entry into the ER. CQ significantly induced phosphorylation of eIF2α in mutant spinal cords (Figure 4), which would inhibit translation. Based on these results, we have proposed a model (Figure 7A) in which CQ effectively inhibits ER stress by blocking ER protein loading. This model is supported by the differential effects of CQ on ER stress related to tunicamycin- or thapsigargin-induced misfolded proteins (Figure 6); tunicamycin induces misfolding of only immature nascent proteins in the ER, whereas thapsigargin induces misfolding of all proteins located in the ER.

In mammals, malaria parasites utilize hemoglobin as a source of amino acids during their erythrocyte stage. The resultant toxic-free heme is detoxified by the parasites' heme polymerase in the acidic digestive vacuoles; however, CQ inhibits heme polymerase[35] and induces cell death in the parasites. CQ also inhibits the function of acidic lysosome in the same manner. Because other lysosome inhibitors did not decrease the amount of msdPLP1-FLAG and eIF2α is not associated with lysosome, we assume that CQ's translation-inhibiting action that attenuates ER-stress is distinct from the lysosome-inhibiting action of CQ. CQ is also used to treat autoimmune and inflammatory diseases, although its mechanisms in these applications are not known.[36] Based on our study, CQ might help against these diseases by inhibiting the translation of autoantibodies or inflammatory cytokines.

Unexpectedly, in contrast to its effect on expression of PLP1 in HeLa cells, CQ was found to significantly upregulate PLP1 and its mRNA in *msd* mice. CQ also increased the expression of the *Mbp* gene, expressed in mature oligodendrocytes, without significantly changing expression of the *Olig02* gene. These results led us to propose the hypothesis illustrated in Figure 7B. *Olig02* is expressed throughout all stages of oligodendrocyte differentiation (Figure 5), whereas PLP1 is expressed only in terminally differentiated oligodendrocytes in wild-type mice (Figure 7Ba and Bb). Oligodendrocyte precursors and pre-oligodendrocytes in *msd* mice differentiate normally in the earlier stages, but fail to differentiate further after the dramatic increase of PLP1 expression (upon terminal maturation), and instead undergo apoptosis as a result of the accumulation of the toxic PLP1 (Figure 7Bc). At the same differentiation step when PLP1 starts to express (square in Figure 7B), CQ effectively downregulates PLP1 expression and promotes survival and further differentiation of premature oligodendrocytes. This creates a slight upregulation in the expression of mature oligodendrocyte marker genes (Figure 7Bd).

Despite the attenuation of ER stress and the upregulation of mature oligodendrocyte markers *in vivo* (Figures 4 and 5), CQ did not prevent the apoptosis of oligodendrocytes in the spinal cords under our experimental conditions. Repeated CQ injections neither prevented disease progression nor prolonged the life span of *msd* mice (data not shown). These findings suggest that the therapeutic effect of CQ is limited to rescuing the lethality of the severe hypomyelinating phenotype of *msd* mice. However, in view of the clear ER stress-attenuating effect of CQ, changing the administration protocol or other modifications may help in pursuing its therapeutic potential *in vivo*.

Like CQ, several other translation inhibitors have been shown to attenuate ER stress *in vitro*.[37,38] One of them, salubrinal, attenuates ER stress by enhancing eIF2α

phosphorylation.[37] It also inhibits ER stress *in vivo*, as found in a mouse model of familial amyotrophic lateral sclerosis.[39] Moreover, a recent study demonstrated that upregulation of CHOP and ATF4 by prolonged ER stress increases translation, ER entry, and cell death,[40] although the effect of CHOP on cell survival in oligodendrocytes may be different from other cells.[41] Interestingly, CQ significantly increases eIF2αphosphorylation in *msd* mice while attenuating ER stress (Figure 4). These observations suggest that CQ activates eIF2α kinase, in addition to an ER stress sensor kinase, PERK. Taken together, the results of these studies strongly suggest that eIF2α may be a key drug target in attenuating ER stress.

In conclusion, we report that CQ reduces the ER stress, caused by a point mutation in the disease-causing *PLP1* gene, by enhancing the phosphorylation of eIF2α and the suppression of cellular translation. This novel pharmacological action suggests that CQ, which is a widely prescribed drug with a well-known therapeutic window and toxicity level in the clinic, may serve as a novel drug for the treatment of PMD and possibly other ER stress-related diseases.

Author contributions: All authors participated in the design, interpretation of the results, analysis of the data, and review of the manuscript; TM conducted experiments and wrote the draft of the manuscript; YN performed biochemical examinations, oligodendrocyte culture, and real time PCR and collected the spinal cords of the mice; SN assisted oligodendrocyte culture; EH maintained mice, performed genotyping, and injected CQ into mice; LG performed statistical analyses; YG and MU revised the final version of the manuscript; KI planned and supervised the entire project, contributed in funding, and revised the manuscript.

ACKNOWLEDGEMENTS

We thank Dr W.B. Macklin (Cleveland Clinic Foundation) for providing *msd* mice, Dr H. Osaka (Kanagawa Children's Medical Center) for providing the human PLP1 genes, Dr M. Itoh (NCNP) for providing PLP1 antibody, Dr T. Inoue (Waseda University) for helping in the image analyses, Dr Y. Matsushima (Kyushu University) for technical advice on pulse-chase experiments, Dr L.T. Reiter (University of Tennessee) for critical comments on this manuscript, and the Central Research Laboratory, Shiga University of Medical Science, for technical support. This study was supported in part by grants from the Heath and Labour Sciences Research Grants, Research on Intractable Diseases (H22-Nanchi-Ippan-132 and H24-Nanchi-Ippan-072, to KI), a Grant from Takeda Science Foundation (to KI), Grants-in-Aid for Scientific Research from the Ministry of Education, Culture, Sports, Science and Technology, Japan (KAKENHI: 21390103 and 23659531, to KI; 23580417, to TM), and Presidential-in-Aid from Shiga University of Medical Science (to TM).

REFERENCES

1. Baumann N, Pham-Dinh D. Biology of oligodendrocyte and myelin in the mammalian central nervous system. *Physioll Rev* 2001;**81**:871–972
2. Pedraza L, Huang JK, Colman DR. Organizing principles of the axoglial apparatus. *Neuron* 2001;**30**:335–44
3. Salzer JL. Polarized domains of myelinated axons. *Neuron* 2003;**40**:297–318
4. Dupouey P, Jacque C, Bourre JM, Cesselin F, Privat A, Baumann N. Immunochemical studies of myelin basic protein in *shiverer* mouse devoid of major dense line of myelin. *Neurosci Lett* 1979;**12**:113–8
5. Klugmann M, Schwab MH, Pühlhofer A, Schneider A, Zimmermann F, Griffiths IR, Nave KA. Assembly of CNS myelin in the absence of proteolipid protein. *Neuron* 1997;**18**:59–70
6. Raskind WH, Williams CA, Hudson LD, Bird TD. Complete deletion of the proteolipid protein gene (PLP) in a family with X-linked Pelizaeus-Merzbacher disease. *Am J Genet* 1991;**49**:1355–60
7. Inoue K, Osaka H, Thurston VC, Clarke JT, Yoneyama A, Rosenbarker L, Bird TD, Hodes ME, Shaffer LG, Lupski JR. Genomic rearrangements resulting in PLP1 deletion occur by nonhomologous end joining and cause different dysmyelinating phenotypes in males and females. *Am J Hum Genet* 2002;**71**:838–53
8. Garbern YH. Pelizaeus-Merzbacher disease: Genetic and cellular pathogenesis. *Cell Mol Life Sci* 2007;**64**:50–65
9. Inoue K. PLP1-related inherited dysmyelinating disorders: Pelizaeus-Merzbacher disease and spastic paraplegia type 2. *Neurogenetics* 2005;**6**:1–16
10. Inoue K, Osaka H, Sugiyama N, Kawanishi C, Onishi H, Nezu A, Kimura K, Yamada Y, Kosaka K. A duplicated PLP gene causing Pelizaeus-Merzbacher disease detected by comparative multiplex PCR. *Am J Hum Genet* 1996;**59**:32–9
11. Inoue K, Osaka H, Imaizumi K, Nezu A, Takanashi J, Arii J, Murayama K, Ono J, Kikawa Y, Mito T, Shaffer LG, Lupski JR. Proteolipid protein gene duplications causing Pelizaeus-Merzbacher disease: molecular mechanism and phenotypic manifestations. *Ann Neurol* 1999;**45**:624–32
12. Roboti P, Swanton E, High S. Differences in endoplasmic-reticulum quality control determine the cellular response to disease-associated mutants of proteolipid protein. *J Cell Sci* 2009;**122**:3942–53
13. Numata Y, Morimura T, Nakamura S, Hirano E, Kure S, Goto YI, Inoue K. Depletion of molecular chaperones from the endoplasmic reticulum and fragmentation of the Golgi apparatus associated with pathogenesis in Pelizaeus-Merzbacher disease. *J Biol Chem* 2013;**288**:7451–66
14. Yoshida H. ER stress and diseases. *FEBS J* 2007;**274**:630–58
15. Gencic S, Hudson LD. Conservative amino acid substitution in the myelin proteolipid protein of *jimpymsd* mice. *J Neurosci* 1990;**10**:117–24
16. Yamamoto T, Nanba E, Zhang H, Sasaki M, Komaki H, Takeshita K. *Jimpy* (*msd*) mouse mutation and connatal Pelizaeus-Merzbacher disease. *Am J Med Genet* 1998;**75**:439–40
17. Fidok DA, Eastman RT, Ward SA, Meshnick SR. Recent highlight in antimalarial drug resistance and chemotherapy research. *Trend Parasitol* 2008;**24**:537–44
18. Morimura T, Hattori M, Ogawa M, Mikoshiba K. Disabled1 regulates the intracellular trafficking of reelin receptors. *J Biol Chem* 2005;**80**:16901–8
19. Krämer-Albers EM, Gehrig-Burger K, Thiele C. Trotter J, Nave KA. Perturbed interactions of mutant proteolipid protein/DM20 with cholesterol and lipid rafts in oligodendroglia: implications for dysmyelination in spastic paraplegia. *J Neurosci* 2006;**26**:1743–52
20. Ishida Y, Nagata K. Autophagy eliminates a specific species of misfolded procollagen and plays a protective role in cell survival against ER stress. *Autophagy* 2009;**5**:1217–9
21. Quin L, Wang Z, Tao L, Wang Y. ER stress negatively regulates AKT/TSC/mTOR pathway to enhance autophagy. *Autophagy* 2010;**6**:239–47
22. Harding HP, Zhang Y, Ron D. Protein translation and folding are coupled by an endoplasmic-reticulum-resident kinase. *Nature* 1999;**397**:271–4
23. Hinnebusch AG. The eIF-2 alpha kinases: regulators of protein synthesis in starvation and stress. *Semin Cell Biol* 1995;**5**:417–26
24. Conasun LM, Potts AM. *In vitro* inhibition of protein synthesis in the retinal pigment epithelium by chloroquine. *Invest Ophthalmol* 1974;**13**:107–15